

AD-B132 565

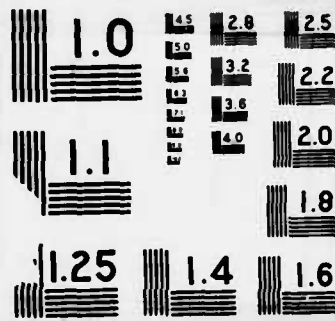
BISTATIC ACOUSTIC SCATTERING: COMPARISON BETWEEN THEORY
AND EXPERIMENT(U) NAVAL SURFACE WARFARE CENTER SILVER
SPRING MD R S HEBBERT ET AL. 10 MAY 88 NSWC/TR-88-142

1/1
USGO
&
CONT

UNCLASSIFIED

F/G 20/1





2

DTIC FILE COPY

NSWC TR 88-142

AD-B132 565

**BISTATIC ACOUSTIC SCATTERING--
COMPARISON BETWEEN THEORY AND
EXPERIMENT**

**BY R. S. HEBBERT AND L. T. BARKAKATI
UNDERWATER SYSTEMS DEPARTMENT**

10 MAY 1988

Distribution authorized to U.S. Government agencies and their contractors only; critical technology (10 May 1988). Other requests shall be referred to NSWC (Code U25), Silver Spring, MD 20903-5000.

DESTRUCTION NOTICE -- For classified documents, follow procedures as outlined in Chapter 17 of OPNAVINST 5510.1H. For unclassified, limited documents, destroy by any method that will prevent disclosure of contents or reconstruction of the document.

DTIC
ELECTE
MAY 17 1989
S H D



NAVAL SURFACE WARFARE CENTER

Dahlgren, Virginia 22448-5000 • Silver Spring, Maryland 20903-5000

89 5 17 028

UNCLASSIFIED

SECURITY CLASSIFICATION OF THIS PAGE

REPORT DOCUMENTATION PAGE

1a. REPORT SECURITY CLASSIFICATION UNCLASSIFIED			1b. RESTRICTIVE MARKINGS			
2a. SECURITY CLASSIFICATION AUTHORITY			3. DISTRIBUTION/AVAILABILITY OF REPORT Distribution is authorized to U.S. Government agencies and their contractors; critical technology (10 May 1988). Other requests shall be referred to NSWC (Code U25), Silver Spring, MD 20903 5000.			
2b. DECLASSIFICATION/DOWNGRADING SCHEDULE			4. PERFORMING ORGANIZATION REPORT NUMBER(S) NSWC TR 88-142			
6a. NAME OF PERFORMING ORGANIZATION Naval Surface Warfare Center			6b. OFFICE SYMBOL (If applicable) U25		5. MONITORING ORGANIZATION REPORT NUMBER(S)	
6c. ADDRESS (City, State, and ZIP Code) White Oak Laboratory 10901 New Hampshire Avenue Silver Spring, MD 20903-5000			7a. NAME OF MONITORING ORGANIZATION			
8a. NAME OF FUNDING/SPONSORING ORGANIZATION			8b. OFFICE SYMBOL (If applicable)		7b. ADDRESS (City, State, and ZIP Code)	
8c. ADDRESS (City, State, and ZIP Code)			9. PROCUREMENT INSTRUMENT IDENTIFICATION NUMBER			
			10. SOURCE OF FUNDING NOS.			
			PROGRAM ELEMENT NO.	PROJECT NO.	TASK NO.	WORK UNIT NO.
11. TITLE (Include Security Classification) Bistatic Acoustic Scattering--A Comparison Between Theory and Experiment						
12. PERSONAL AUTHOR(S) Hebbert, R. S., and Barkakati, L. T.						
13a. TYPE OF REPORT Final		13b. TIME COVERED FROM TO		14. DATE OF REPORT (Yr., Mo., Day) 1988, May, 10		15. PAGE COUNT 31
16. SUPPLEMENTARY NOTES						
17. COSATI CODES			18. SUBJECT TERMS (Continue on reverse if necessary and identify by block number)			
FIELD	GROUP	SUB. GR.				
20	01		Acoustic Electromagnetic waves Scattering, (jnd) e			
			Kirchhoff approximation Scalar Waves			
19. ABSTRACT (Continue on reverse if necessary and identify by block number) <p>This report presents three methods of solving the problem of acoustic scattering from deterministic underwater bodies. The first method uses the exact solution to the wave equation that matches the prescribed boundary conditions at the obstacle (scatterer). This can be readily obtained only for a cylinder or sphere and, in less general form, for an ellipsoid. The second approach is to use a technique called the Kirchhoff approximation which is applicable when the wavelength of sound is small compared to the dimensions of the scatterer. The third recourse is to take measurements when this is possible. In this report examples of all three approaches are given. In particular, it is found that, for spherical and conical shapes, most of the scattered energy is confined to a cone in the forward direction.</p> <p><i>Keywords:</i></p>						
20. DISTRIBUTION AVAILABILITY OF ABSTRACT <input type="checkbox"/> UNCLASSIFIED/UNLIMITED <input checked="" type="checkbox"/> SAME AS RPT <input type="checkbox"/> DTIC USERS			21. ABSTRACT SECURITY CLASSIFICATION UNCLASSIFIED			
22a. NAME OF RESPONSIBLE INDIVIDUAL L. T. Barkakati			22b. TELEPHONE NUMBER (Include Area Code) (202) 394-1218		22c. OFFICE SYMBOL U25	

UNCLASSIFIED

SECURITY CLASSIFICATION OF THIS PAGE

THIS PAGE IS INTENTIONALLY BLANK

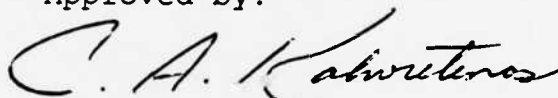
UNCLASSIFIED

SECURITY CLASSIFICATION OF THIS PAGE

FOREWORD

This tutorial report should help others in the laboratory to understand and to use the Kirchhoff technique in analyzing sound scattered by underwater bodies. The technique is well documented in the existing literature, but this thorough presentation of its use in the context of underwater acoustic scattering makes the report valuable.

Approved by:



C. A. KALIVRETENOS, Head
Sensors and Electronics Division



Accession For	
NTIS GRA&I	<input type="checkbox"/>
DTIC TAB	<input checked="" type="checkbox"/>
Unannounced	<input type="checkbox"/>
Justification	
By _____	
Distribution/	
Availability Codes	
Dist	Avail and/or Special
<i>C-2</i>	

CONTENTS

<u>Section</u>		<u>Page</u>
1	INTRODUCTION	1
2	EXPERIMENTAL SETUP	3
3	RESULTS	5
4	CONCLUSIONS	7
	DISTRIBUTION.....	(1)

<u>Appendix</u>		<u>Page</u>
A	EXACT SOLUTION FOR SCATTERING FROM A LIQUID SPHERE	A-1
B	THE KIRCHHOFF SCATTERING APPROXIMATION	B-1

ILLUSTRATIONS

<u>Figure</u>		<u>Page</u>
1	BISTATIC, MONOSTATIC, AND FORWARD SCATTERING . . .	9
2	GEOMETRY OF THE EXPERIMENT	10
3	MEASUREMENT OF SCATTERING FROM A SPHERE AT 50 KHZ	10
4	MEASUREMENT OF SCATTERING FROM A SPHERE AT 125 KHZ	10
5	PREDICTED MEASUREMENT FROM THE KIRCHHOFF APPROXIMATION AND FROM THE EXACT SOLUTION FOR THE SPHERE AT 50 KHZ	10
6	MEASUREMENT OF SCATTERING FROM A CONE AT 50 KHZ	11
7	PREDICTED MEASUREMENT FROM THE KIRCHHOFF APPROXIMATION FOR THE CONE AT 50 KHZ	11
8	EXACT SOLUTION FOR SOFT SPHERES OF RADII 2 λ AND 4 λ	11
9	EXACT SOLUTION FOR RIGID SPHERES OF RADII 2 λ AND 4 λ	11
10	EXACT SOLUTION FOR LIQUID SPHERES OF RADII 2 λ AND 4 λ WITH A SMALL IMPEDANCE MISMATCH	11
11	EXACT SOLUTION FOR LOSSY SPHERES OF RADII 2 λ AND 4 λ	11
12	SCATTERING FROM A CYLINDER WITH HEMISPHERICAL END CAPS BY THE KIRCHHOFF METHOD	12
13	SCATTERING FROM A SOFT SPHERE AND A SPHERICAL SHELL OF ALUMINUM AT ITS RESONANT FREQUENCY	12
14	SCATTERING FROM A SOFT SPHERE AND A SPHERICAL SHELL OF ALUMINUM AT FREQUENCY 10% HIGHER THAN ITS RESONANT FREQUENCY	12
15	SCATTERING FROM A SOFT SPHERE AND A SPHERICAL SHELL OF ALUMINUM AT FREQUENCY 10% LOWER THAN ITS RESONANT FREQUENCY	12
16	BACK SCATTER AMPLITUDE VERSUS FREQUENCY FOR THE SPHERICAL SHELL	13
B-1	INCIDENT, REFLECTED, AND TRANSMITTED WAVES IN SCATTERING FROM A HALF-PLANE	B-8

SECTION 1

INTRODUCTION

Active detection and tracking of underwater targets requires knowledge of how they reflect sound waves. For this reason, the Navy has a continuing interest in acoustic scattering. Acoustic or sound wave scattering refers to the way a pressure wave bounces off obstacles in its path. We consider a source, a scatterer, and a receiver which monitor the direct signal and the signal scattered from the obstacle. There are two types of scattering depending on where the sound waves are observed. If the source and the observation points are one and the same, the problem is one of monostatic scattering. Radars (in the electromagnetic case) and active sonars usually operate this way. When the source and the observation points are not coincident, we call it bistatic scattering (see Figure 1). Monostatic scattering is simply a special case of the bistatic problem. When the target lies close to the line joining the source and the observation points, the problem is one of forward scattering. In this report we will consider the general case of bistatic scattering and in certain sections emphasize forward scattering.

Unlike electromagnetic waves, the acoustic pressure waves are scalar and their study is somewhat simpler than that of their electromagnetic counterpart. The exact solution to the problem of scattering of a scalar wave from a sphere was obtained as early as 1863 by Clebsch. By 1890, the scattering from ellipsoids was solved as well. These shapes were tractable because they are amenable to the technique of separation of variables which involves using a coordinate frame where the field can be expressed as a product of functions that depend on individual coordinates. However, no other bounded shape allows the use of this technique. All subsequent solution techniques rely on approximations and series expansions of various kinds.

The approximations are based on the interrelationship of the parameters of the scattering problem: the wavelength of the sound wave, the maximum physical dimension of the scatterer and the distances of the source and observation points from the scatterer. Typically, the source and

observation points are assumed to be located far (compared to the wavelength) from the scatterer.

We will next describe the experimental setup used to obtain the measurements of scattered field. We will then explain the validation of the measurements by using the sphere as an example. We will also present theoretical as well as measured results for scattering from several interesting bodies.

The theoretical derivations appear in two appendices. In Appendix A, we derive the exact solution to the problem of acoustic scattering from a liquid sphere. Appendix B contains the derivation of Kirchhoff approximation applied to bistatic scattering of scalar waves. Using the sphere as an example, we have elaborated the conditions under which the Kirchhoff approximation holds well.

SECTION 2

EXPERIMENTAL SETUP

The experiment was conducted in the Naval Surface Warfare Center (NSWC) Hydroacoustic Facility which uses a tank 20-feet deep and 30-feet in diameter. The source, scatterer, and receiver were placed at a depth of 10 feet. Two E27 transducers were used as the source and the receiver. The actual geometry of the experiment is shown in Figure 2. The source emits a long pulse with a duration of 1 to 2 msec, i.e., 5 to 10 feet in length. A time gate was used to observe both direct and scattered pulses. This, in effect, gives a continuous wave system but without reflections from the walls of the tank.

The experiment was done on two styrofoam objects: a frustum of a cone with its axis oriented vertically and a sphere. The styrofoam sphere was 4 inches in diameter. The frustum of the cone was 6-inches high, with diameters of 0.75 inch at one end and 2.5 inches at the other. The measurements were made at two frequencies: 50 kHz and 125 kHz.

Validation of Measurements

The experiment was validated by comparing the measurements for scattering from the soft styrofoam sphere with the exact solution for this problem. As shown in Figures 3 and 4, the experimental results match well with the theoretical values.

SECTION 3

RESULTS

The measurements from the NSWC Hydroacoustic Facility, shown in Figures 3, 4, and 6, display the total received power (in dB) in a polar plot. The total received power is the magnitude of the complex sum of the direct and scattered waves at the receiver. In the polar plots, the angle corresponds to the angular location of the receiver relative to the line joining the source and the scatterer.

Figure 3 shows the scattering at 50 kHz from a styrofoam sphere with a diameter of 4 inches. Figure 4 shows measurements for the same sphere at 125 kHz. At 125 kHz, the transducer generates a very narrow beam so the pattern drops off rapidly as we move out of the -30° to $+30^\circ$ zone in azimuth. However, within this zone the experimental results agree well with the theory. Figure 5 displays the predicted results for the sphere from both the exact solution and the Kirchhoff approximation. Note that the discrepancy in the forward direction is exaggerated because of an approximation we used when evaluating the field predicted by the Kirchhoff approach.

Figures 6 and 7, respectively, show measurements from the frustum of a cone and the values predicted by the Kirchhoff approximation. The computation of the field predicted by the Kirchhoff approximation was handled properly in this case. Hence, the discrepancy is reduced in the forward direction between the measured and predicted fields.

The next two figures show polar plots for calculated bistatic scattering from spheres of radii 2 and 4 wavelengths. Figure 8 is for soft spheres and Figure 9 for rigid spheres. Figures 10 and 11 show calculated bistatic scattering from liquid spheres containing a fluid whose density is the same as that of the fluid outside. In Figure 10, the speed of sound inside the sphere is slightly less than that in the surrounding medium. In Figure 11, the density as well as the speed of sound are the same inside and out, but the interior fluid has a small loss (a black sphere).

Figure 12 shows the calculated results of bistatic scattering from a cylinder with hemispherical end caps as calculated by the Kirchhoff method. The cylinder is 12-wavelengths long by 2-wavelengths in diameter. The concentric circles represent 10db steps. The forward peak is normalized with respect to the outer circle. Note that the specular reflection (at 30°) is about 10db down from the forward scattered power. Calculations were also made for bistatic scattering from cylindrical and spherical metal shells. It is well known that these structures show resonances in the backscattered amplitude. However, these resonances are much less pronounced in the forward scattered field. In fact, the forward scatter for spheres and cylinders with thin shells is very similar to that for a soft scatterer. Figure 13 shows the calculated results of scattering from a spherical shell of aluminum with thickness 0.01 times the radius at the resonant frequency. On the same figure, we also show the scattering from a soft sphere to emphasize the similarity in forward scatter from the two scatterers. Figures 14 and 15 displays the calculated results for the same problem at frequencies 10 percent higher and 10 percent lower than the resonant frequency. Figure 16 shows the backscatter amplitude versus frequency for the same spherical shell of aluminum.

SECTION 4

CONCLUSIONS

In this report, we described the use of the Kirchhoff approximation technique to solve for the forward acoustic scattering from several shapes. We found that regardless of the composition of the scatterer, soft, rigid, or resonant shell, there is always a strong forward scatter signal. In the $\pm 30^\circ$ azimuthal zone, the shape of this forward scatter pattern can be computed, with good accuracy, by using the Kirchhoff approximation to solve the Helmholtz integral equation subject to the appropriate boundary conditions. We also found that the backward scattering can be reduced at some frequencies; however, the forward scatter energy also exists at all frequency.

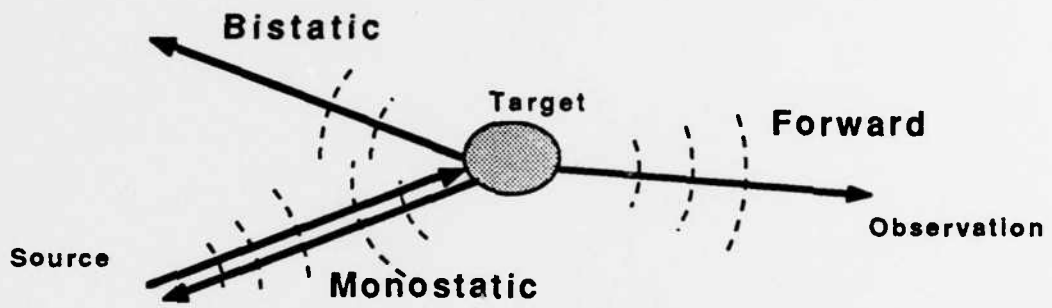


FIGURE 1. BISTATIC, MONOSTATIC, AND FORWARD SCATTERING

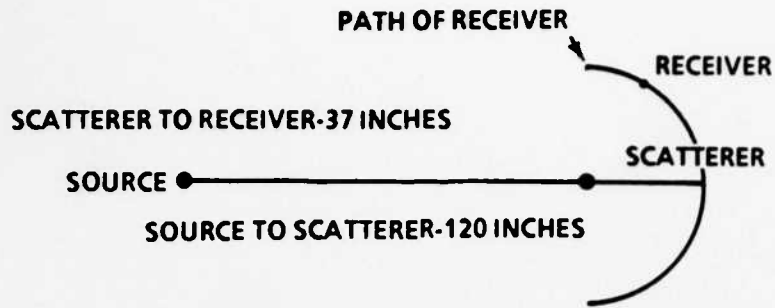


FIGURE 2. GEOMETRY OF THE EXPERIMENT

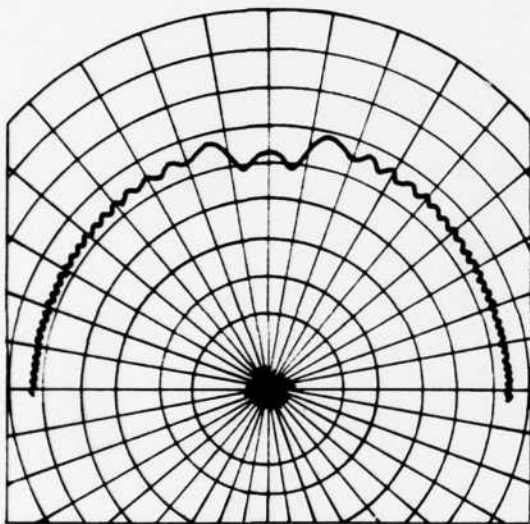


FIGURE 3. MEASUREMENT OF SCATTERING FROM A SPHERE AT 50HZ

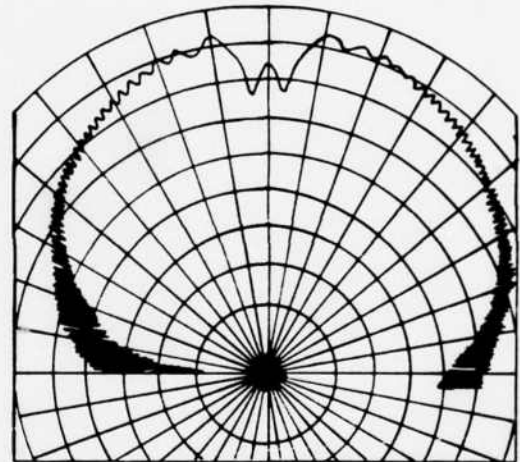


FIGURE 4. MEASUREMENT OF SCATTERING FROM A SPHERE AT 125HZ

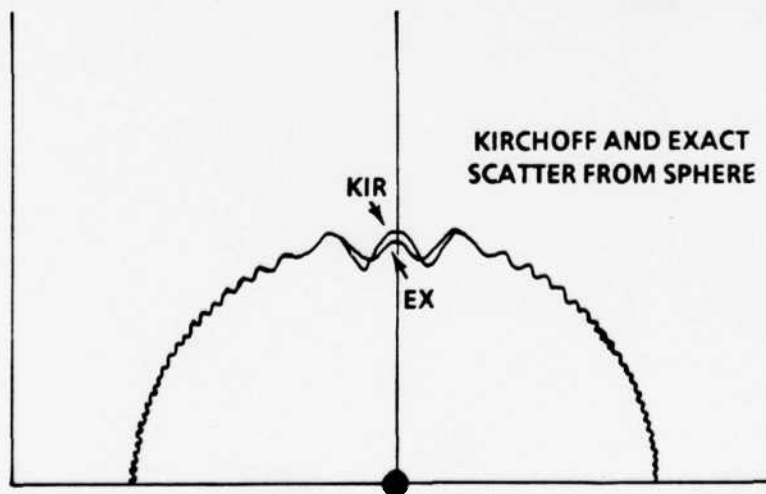


FIGURE 5. PREDICATED MEASUREMENT FROM THE KIRCHHOFF APPROXIMATION AND FROM THE EXACT SOLUTION FOR THE SPHERE AT 50HZ

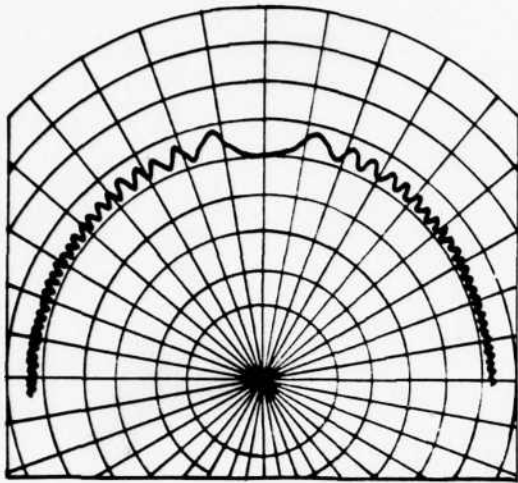


FIGURE 6. MEASUREMENT OF SCATTERING FROM A CONE AT 50HZ

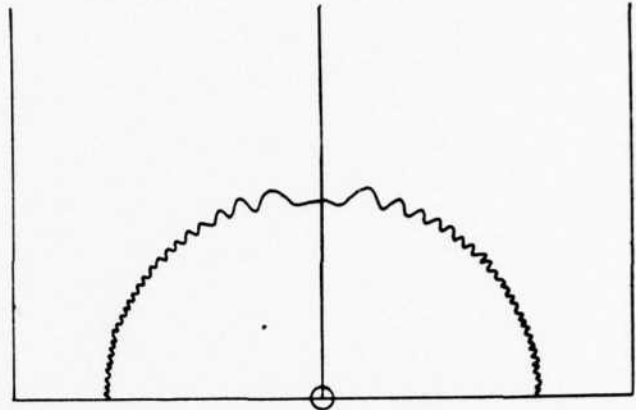


FIGURE 7. PREDICATED MEASUREMENT FROM THE KIRCHHOFF APPROXIMATION FOR THE CONE AT 50HZ

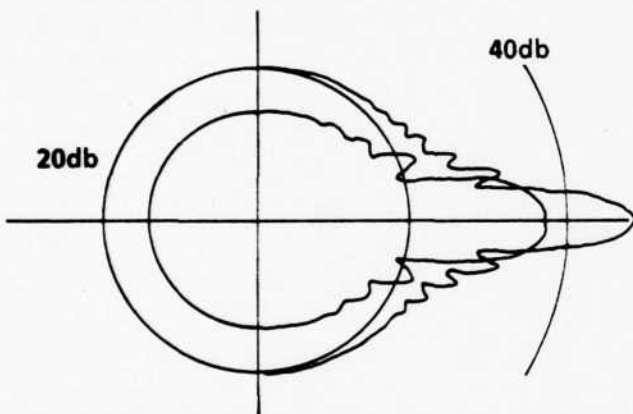


FIGURE 8. EXACT SOLUTION FOR SOFT SPHERES OF RADII 2λ AND 4λ

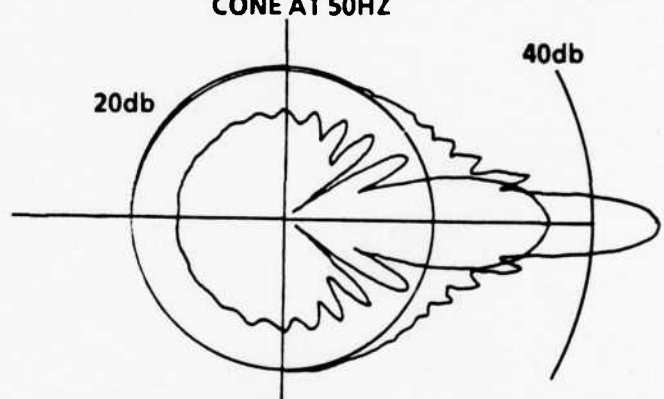


FIGURE 9. EXACT SOLUTION FOR RIGID SPHERES OF RADII 2λ AND 4λ

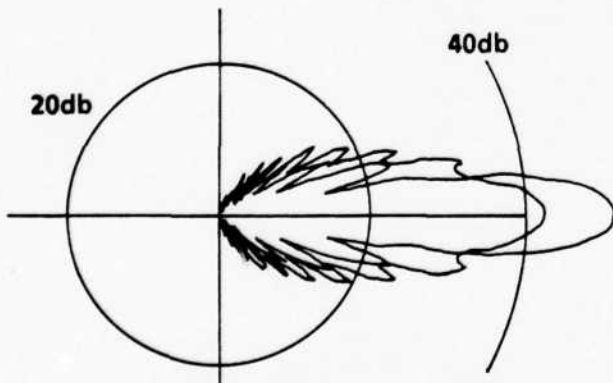


FIGURE 10. EXACT SOLUTION FOR LIQUID SPHERES OF RADII 2λ AND 4λ WITH A SMALL IMPEDANCE MISMATCH

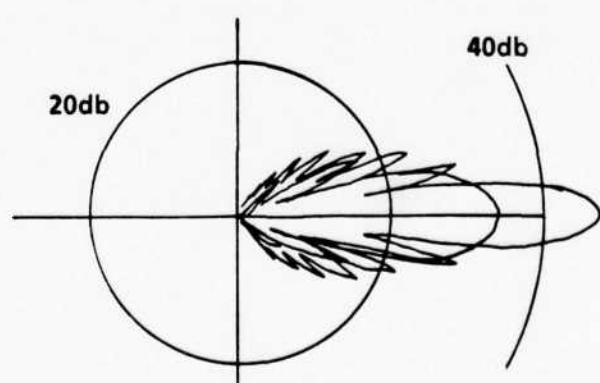


FIGURE 11. EXACT SOLUTION FOR LOSSY SPHERES OF RADII 2λ AND 4λ

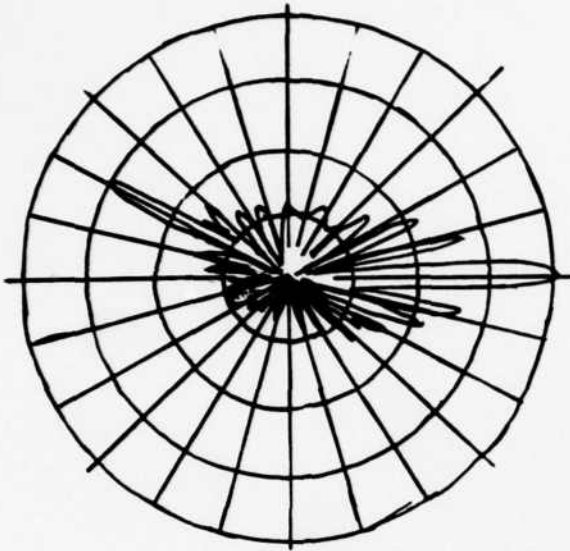


FIGURE 12. SCATTERING FROM A CYLINDER WITH HEMISPHERICAL END CAPS BY THE KIRCHHOFF METHOD

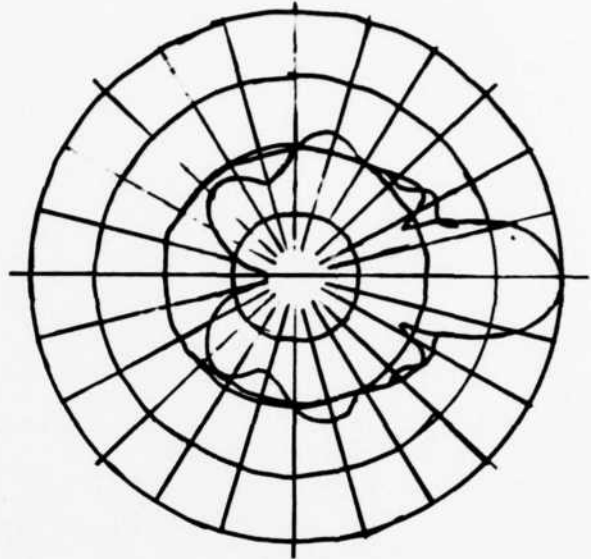


FIGURE 13. SCATTERING FROM A SOFT SPHERE AND A SPHERICAL SHELL OF ALUMINUM AT RESONANT FREQUENCY

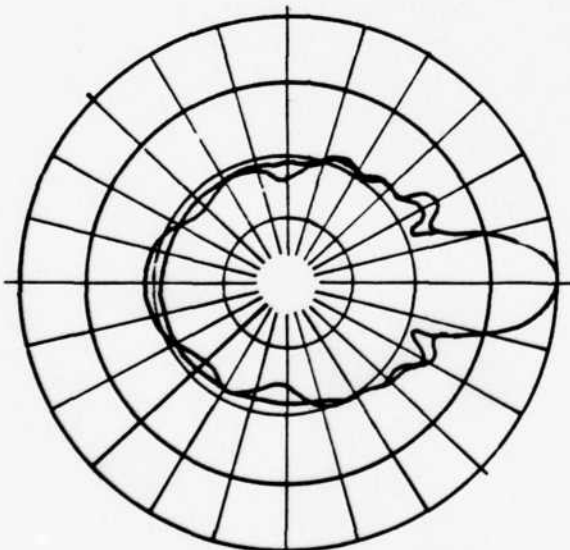


FIGURE 14. SCATTERING FROM A SOFT SPHERE AND A SPHERICAL SHELL OF ALUMINUM AT FREQUENCY 10% HIGHER THAN ITS RESONANT FREQUENCY

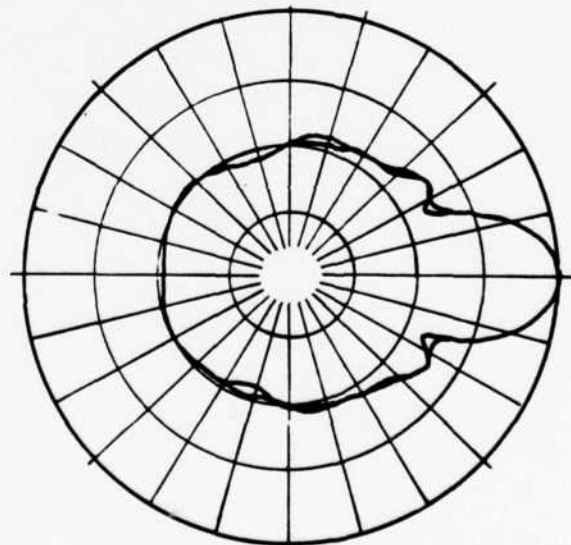


FIGURE 15. SCATTERING FROM A SOFT SPHERE AND A SPHERICAL SHELL OF ALUMINUM AT FREQUENCY 10% LOWER THAN ITS RESONANT FREQUENCY

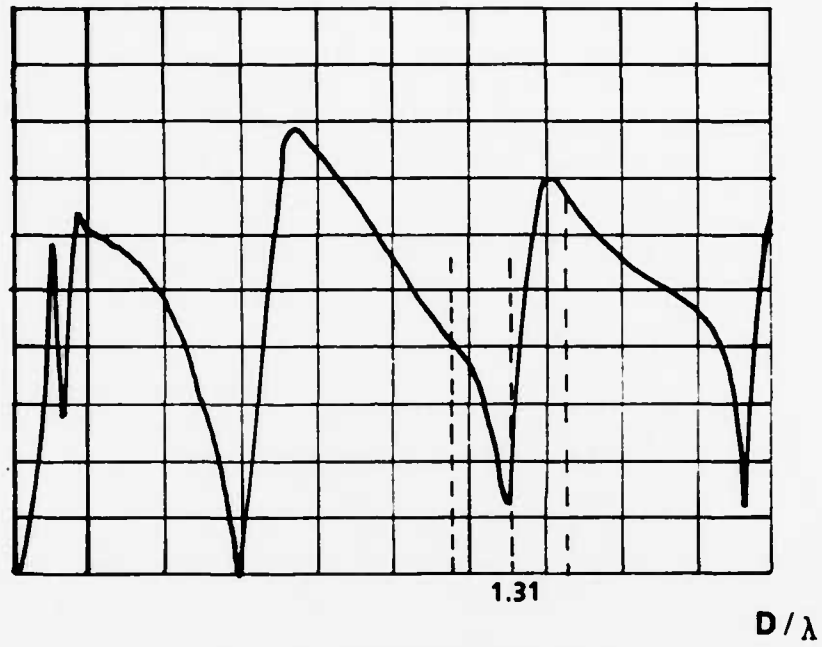


FIGURE 16. BACK SCATTER AMPLITUDE VERSUS FREQUENCY FOR THE SPHERICAL SHELL

APPENDIX A

EXACT SOLUTION FOR SCATTERING FROM A LIQUID SPHERE

Consider a plane wave propagating along the z-axis. Suppose this wave impinges on a liquid sphere of radius a at the origin. Let the point of observation be at (R, θ) in spherical coordinates. Let Ψ , Ψ_I and Ψ_S be the total field, the incident field and the scattered field, respectively. Thus, we have

$$\Psi = \Psi_I + \Psi_S$$

Since the incident plane wave is propagating along the z-axis, we get (see Reference A-1)

$$\begin{aligned} \Psi_I &= e^{ikz} = e^{ikr\cos\theta} \\ &= \sum_{n=0}^{\infty} a_n j_n(kr) P_n(\cos\alpha) \end{aligned} \quad (\text{A-1})$$

where $j_n(x) = \sqrt{\frac{\pi}{2x}} J_{n+\frac{1}{2}}(x)$, $J_q(x)$ is the Bessel function, and $P_n(\cos\alpha)$ is the Legendre polynomial.

A-1

Stratton, J. A., Electromagnetic Theory, McGraw-Hill Book Co., Inc., New York, NY, 1941, pp. 408-409.

Multiplying both sides of Equation (A-1) by $P_i(\cos\alpha)\sin\alpha$ and integrating with respect to α , we get

$$\frac{2}{2i+1} a_i j_i(kr) = \int_0^\pi e^{ikr\cos\alpha} P_i(\cos\alpha)\sin\alpha \, d\alpha \quad (\text{A-2})$$

If we let $x \equiv kr$, we can show that

$$\left(\frac{d^n j_n(x)}{dx^n} \right)_{x=0} = \frac{2^n (n!)^2}{(2n+1)!}$$

and hence,

$$\frac{2^n (n!)^2}{(2n+1)!} a_n = \frac{2n+1}{2} i^n \int_0^\pi \cos^n \alpha P_n(\cos\alpha)\sin\alpha \, d\alpha \quad (\text{A-3})$$

Let $I_n = \int_0^\pi \cos^n \alpha P_n(\cos\alpha)\sin\alpha \, d\alpha$. Then, integrating I_n

by parts, we get

$$\begin{aligned} nI_n &= -(n+1)I_n + nI_{n-1} \\ I_n &= \frac{n}{2n+1} I_{n-1} \end{aligned}$$

Substituting the value of I_0, I_1, I_2, \dots , and using induction we get

$$I_n = \frac{2^{n+1} (n!)^2}{(2n+1)!}$$

Therefore,

$$a_n = (2n+1) i^n$$

$$\Psi_I = \sum_{n=0}^{\infty} i^n (2n+1) j_n(kr) P_n(\cos\alpha) \quad (\text{A-4})$$

Since the scattered field outside the sphere consists of outgoing waves at distances far from the sphere, we write

$$\Psi_S = \sum_{n=0}^{\infty} c_n h_n^{(1)}(kr) P_n(\cos\alpha) \quad (\text{A-5})$$

where $h_n^{(1)} = j_n + iy_n$. Inside the sphere, the field is

$$\Psi = \Psi_S = \sum_{n=0}^{\infty} b_n j_n(kr) P_n(\cos\alpha)$$

At the boundary of the sphere, the pressure inside must be equal to the pressure outside. Therefore,

$$\begin{aligned} & \sum_{n=0}^{\infty} [i^n (2n+1) j_n(ka) + c_n h_n^{(1)}(ka)] P_n(\cos\alpha) \\ &= \sum_{n=0}^{\infty} b_n j_n(ka) P_n(\cos\alpha) \end{aligned} \quad (\text{A-6})$$

or,

$$[i^n (2n+1) j_n(ka) + c_n h_n^{(1)}(ka)] = b_n j_n(ka) \quad (\text{A-7})$$

Let ρ_1 and k_1 , respectively, be the density and the propagation constant inside the sphere. Let ρ_2 and k_2 be the corresponding quantities outside the sphere. Let $V(r)^{(1)}$ and $V(r)^{(2)}$, respectively, be the radial velocities inside and outside the sphere. Applying the boundary conditions for the radial velocities, we obtain

$$v(a)^{(1)} = v(a)^{(2)} \quad \text{and} \quad v(r) = \frac{1}{i\omega\rho} \frac{\partial p}{\partial r}$$

Hence,

$$\frac{k_1}{\rho_1} b_n j_n'(ka) = \frac{k_2}{\rho_2} [i^n(2n+1) j_n'(ka) + c_n h_n^{(1)'}(ka)]$$

or,

$$c_n = \frac{i^n(2n+1) [z_1 j_n'(x_1) j_n(x_2) - z_2 j_n(x_1) j_n'(x_2)]}{z_2 j_n(x_1) h_n'(x_2) - z_1 j_n'(x_1) h_n(x_2)} \quad (\text{A-8})$$

where $z_1 = k_1 \rho_2$, $z_2 = k_2 \rho_1$, $x_1 = k_1 a$, and $x_2 = k_2 a$. Note that the propagation constant need not be real inside the sphere. When the propagation constant, k_1 , is complex, we say that the sphere is lossy.

For a soft sphere, $\rho_2 = 1$ and $\rho_1 = 0$. In this case, we get

$$c_n = -i^n(2n+1) \frac{j_n(x_2)}{h_n(x_2)}. \quad (\text{A-9})$$

For a rigid sphere, $\frac{\rho_2}{\rho_1} \rightarrow 0$. In this case,

$$c_n = i^n(2n+1) \frac{j_n'(x_2)}{h_n'(x_2)}. \quad (\text{A-10})$$

APPENDIX B

THE KIRCHHOFF SCATTERING APPROXIMATION

In this section we will apply the Kirchhoff approximation to acoustic scattering. First, we will derive the integral form of the wave equation by using the divergence theorem. Then we will show how to obtain an approximate solution of the integral equation by using the Kirchhoff approximation.

The divergence theorem states that

$$\int_v dv \nabla \cdot \underline{f} = \int_s da \underline{f} \cdot \underline{n} \quad (\text{B-1})$$

provided \underline{f} has no singularities within v . Here, ∇ is the divergence of a vector and \underline{n} is the outward normal to the surface.

Now consider a system with a unity source at \underline{a} , a scatterer bounded by surface S_s , and a point of observation \underline{r} . The source may be described by

$$\frac{e^{ik|\underline{r} - \underline{a}|}}{|\underline{r} - \underline{a}|}$$

We wish to find $\phi(\underline{r})$ where $\nabla^2 \phi + k^2 \phi = 0$ and appropriate boundary conditions are satisfied on S_s .

Let us define an auxiliary function $G \equiv \frac{e^{ik|\mathbf{r}' - \mathbf{r}|}}{|\mathbf{r}' - \mathbf{r}|}$ and $\mathbf{f} \equiv G\nabla\phi - \phi\nabla G$. Note that G satisfies the wave equation except at $\mathbf{r}' = \mathbf{r}$.

We will now apply the divergence theorem on \mathbf{f}

$$\begin{aligned}\nabla \cdot \mathbf{f} &= \nabla G \cdot \nabla \phi + G \nabla^2 \phi - \nabla \phi \cdot \nabla G - \phi \nabla^2 G \\ &= -k^2 G \phi + k^2 G \phi = 0\end{aligned}\quad (\text{B-2})$$

Therefore,

$$\int_V dv \nabla \cdot \mathbf{f} = 0 = \int_S da \mathbf{f} \cdot \mathbf{n} \quad (\text{B-3})$$

Since V must be a volume free of singularities, we must exclude the singularities at the source position \mathbf{a} and the observation position \mathbf{r} from the volume. Let V be the interior to surface S_∞ , a sphere whose radius is indefinitely large and exterior to S_S, S_a, S_r , where S_a and S_r are spheres of indefinitely small radius, centered at the source \mathbf{a} and the observation point \mathbf{r} respectively.

Then from Equation (B-3), we get

$$\int_{S_I} da \mathbf{f} \cdot \mathbf{n} + \int_{S_a} da \mathbf{f} \cdot \mathbf{n} + \int_{S_r} da \mathbf{f} \cdot \mathbf{n} + \int_{S_S} da \mathbf{f} \cdot \mathbf{n} = 0 \quad (\text{B-4})$$

$$\mathbf{f} \cdot \mathbf{n} = G \nabla \phi \cdot \mathbf{n} - \phi \nabla G \cdot \mathbf{n} = G \frac{\partial \phi}{\partial n} - \phi \frac{\partial G}{\partial n} \quad (\text{B-5})$$

Over the spheres S_a and S_r the positive normal is directed radially towards the center, or, out of the volume V .

Therefore

$$\frac{\partial \phi}{\partial n} = - \frac{\partial \phi}{\partial r} .$$

Hence,

$$\underline{f} \cdot \underline{n} = - \frac{e^{ik|r' - r|}}{|r' - r|} \frac{\partial \phi}{\partial r} - \phi \frac{\partial}{\partial n} \left\{ \frac{e^{ik|r' - r|}}{|r' - r|} \right\} \quad (\text{B-6})$$

Now consider

$$\int_{S_a} \text{d}a \underline{f} \cdot \underline{n} = - \int_a \frac{e^{ik|r' - r|}}{|r' - r|} \frac{\partial \phi}{\partial r} - \phi \frac{\partial}{\partial n} \left\{ \frac{e^{ik|r' - r|}}{|r' - r|} \right\} \quad (\text{B-7})$$

where G and $\frac{\partial G}{\partial n}$ are bounded over S_a , and ϕ is the sum of the scattered field and the source field. The scattered field is also bounded. The source is of the order $\frac{1}{r}$ and $\frac{\partial \phi}{\partial n}$ is of the order $\frac{1}{r^2}$. The surface area of S_a is $4\pi r^2$. As r , the radius of S_a , is allowed to vanish, the contribution of the sphere to right hand side of Equation (B-7) is

$$\int_{S_a} \text{d}a \underline{f} \cdot \underline{n} = 4\pi r^2 \frac{e^{ik|r - a|}}{|r - a|} \frac{1}{r^2} = 4\pi \frac{e^{ik|r - a|}}{|r - a|} \quad r \rightarrow 0$$

Similarly with $\int_{S_r} \text{d}a \underline{f} \cdot \underline{n}$, ϕ and $\frac{\partial \phi}{\partial r}$ are bounded over S_r . G is of the order $\frac{1}{r}$ and $\frac{\partial G}{\partial n}$ is of the order $\frac{1}{r^2}$. Hence,

$$\int_{S_r} da \underline{f} \cdot \underline{n} = -4\pi\phi(\underline{r})$$

On S_∞ , let the radius $R \rightarrow \infty$. The area of S_∞ is $4\pi R^2$,

$G \frac{\partial \phi}{\partial n}$ and $\phi \frac{\partial G}{\partial n}$ can be written as

$$G \frac{\partial \phi}{\partial n} = \frac{a}{r^2} + \frac{b}{r^3} + \dots$$

$$\phi \frac{\partial G}{\partial n} = \frac{a}{r^2} + \frac{c}{r^3} + \dots$$

Hence,

$$\int_{S_\infty} da \underline{f} \cdot \underline{n} \rightarrow 0 \text{ as } R \rightarrow \infty.$$

Thus, collecting terms, we obtain

$$\int_{S_\infty + S_r + S_a + S_s} da \underline{f} \cdot \underline{n} = 0 = 4\pi \frac{e^{ik|\underline{r} - \underline{a}|}}{|\underline{r} - \underline{a}|} - 4\pi\phi(\underline{r}) + \int_{S_s} da \underline{f} \cdot \underline{n} \quad (\text{B-8})$$

$$\phi(\underline{r}) = \frac{e^{ik|\underline{r} - \underline{a}|}}{|\underline{r} - \underline{a}|} + \frac{1}{4\pi} \int_{S_s} da \underline{f} \cdot \underline{n} \quad (\text{B-9})$$

Here \underline{n} is the inward normal. If we replace this with the usual outward normal, we get

$$\phi(\underline{r}) = \frac{e^{ik|\underline{r} - \underline{a}|}}{|\underline{r} - \underline{a}|} - \frac{1}{4\pi} \int_{S_S} da G \frac{\partial \phi}{\partial n} - \phi \frac{\partial G}{\partial n} \quad (\text{B-10})$$

This is referred to as Helmholtz's second theorem. While formally correct, it is an integral equation for ϕ and not useful for computation without certain approximations.

The Kirchhoff approximation to the Helmholtz integral assumes that the radius of curvature at every point on the surface is large compared to the wavelength. The scatterer itself can be either soft or rigid. To apply the Kirchhoff approximation, we have to derive the boundary conditions for ϕ and $\frac{\partial \phi}{\partial n}$ when the radius of curvature of the surface becomes large compared to the wavelength. This is the same as the boundary conditions for scattering from the half plane. We derive these boundary conditions next.

Let ϕ_I , ϕ_R and ϕ_T be the incident, reflected and transmitted fields (see Figure B-1), respectively, given by

$$\begin{aligned} \phi_I &= e^{ik_1(x\cos\theta + y\sin\theta)} \\ \phi_R &= \alpha e^{ik_1(-x\cos\theta + y\sin\theta)} \\ \phi_T &= \beta e^{ik_2(x\cos\eta + y\sin\eta)} \end{aligned}$$

At $x = 0$ we have

$$\phi_I + \phi_R = \phi_T \quad (\text{B-11})$$

Hence,

$$(1 + \alpha) e^{ik_1 y \sin\theta} = \beta e^{ik_2 y \sin\eta}$$

or,

$$\beta = (1+\alpha) \quad \text{and} \quad k_1 \sin\theta = k_2 \sin\eta$$

The velocity also has to match at the boundary, $x=0$, thus,

$$\frac{1}{i\omega\rho_2} \frac{\partial\phi_T}{\partial x} = \frac{1}{i\omega\rho_1} \frac{\partial\phi_I}{\partial x} + \frac{1}{i\omega\rho_1} \frac{\partial\phi_R}{\partial x} \quad (\text{B-12})$$

$$\frac{\partial\phi_I}{\partial x} = i\beta k_2 \cos\eta e^{ik_2 y \sin\eta} \quad (\text{B-13})$$

$$\frac{\partial\phi_I}{\partial x} + \frac{\partial\phi_R}{\partial x} = ik_1 \cos\theta (1-\alpha) e^{ik_1 y \sin\theta} \quad (\text{B-14})$$

Combining Equations (B-11), (B-12), and (B-13), we get

$$\frac{k_1}{\rho_1} \cos\theta (1-\alpha) e^{ik_1 y \sin\theta} = \frac{k_2}{\rho_2} \beta \cos\eta e^{ik_2 y \sin\eta}$$

or,

$$\begin{aligned} \beta &= \left(\frac{k_1}{k_2}\right) \left(\frac{\rho_1}{\rho_2}\right) \frac{\cos\theta}{\cos\eta} (1-\alpha) \\ &= \left(\frac{k_1}{k_2}\right) \left(\frac{\rho_1}{\rho_2}\right) \frac{\cos\theta}{\sqrt{k_2^2 - k_1^2 \sin^2\theta}} (1-\alpha) \end{aligned}$$

or,

$$\alpha = \frac{\rho_2 k_1 \cos\theta - \rho_1 \sqrt{k_2^2 - k_1^2 \sin^2\theta}}{\rho_2 k_1 \cos\theta + \rho_1 \sqrt{k_2^2 - k_1^2 \sin^2\theta}}$$

At $x = 0$, $\phi_T = (1+\alpha)\phi_I$. Since
 for soft scatterer, $\rho_2 \rightarrow 0$, $\alpha \rightarrow -1$, and
 for rigid scatterer, $\rho_2 \rightarrow \infty$, $\alpha \rightarrow 1$.

Hence,

$\phi_T = 0$ for an infinitely soft scatterer, and

$\phi_T = 2\phi_I$ for an infinitely rigid scatterer.

At $x = 0$, $\frac{\partial\phi_T}{\partial n} = (1-\alpha)\frac{\partial\phi_I}{\partial n}$

Hence,

$\frac{\partial\phi_T}{\partial n} = 2\frac{\partial\phi_I}{\partial n}$ for soft scatterer

$\frac{\partial\phi_T}{\partial n} = 0$ for rigid scatterer

These boundary conditions, when used on the Helmholtz equation, constitute the Kirchhoff approximation.

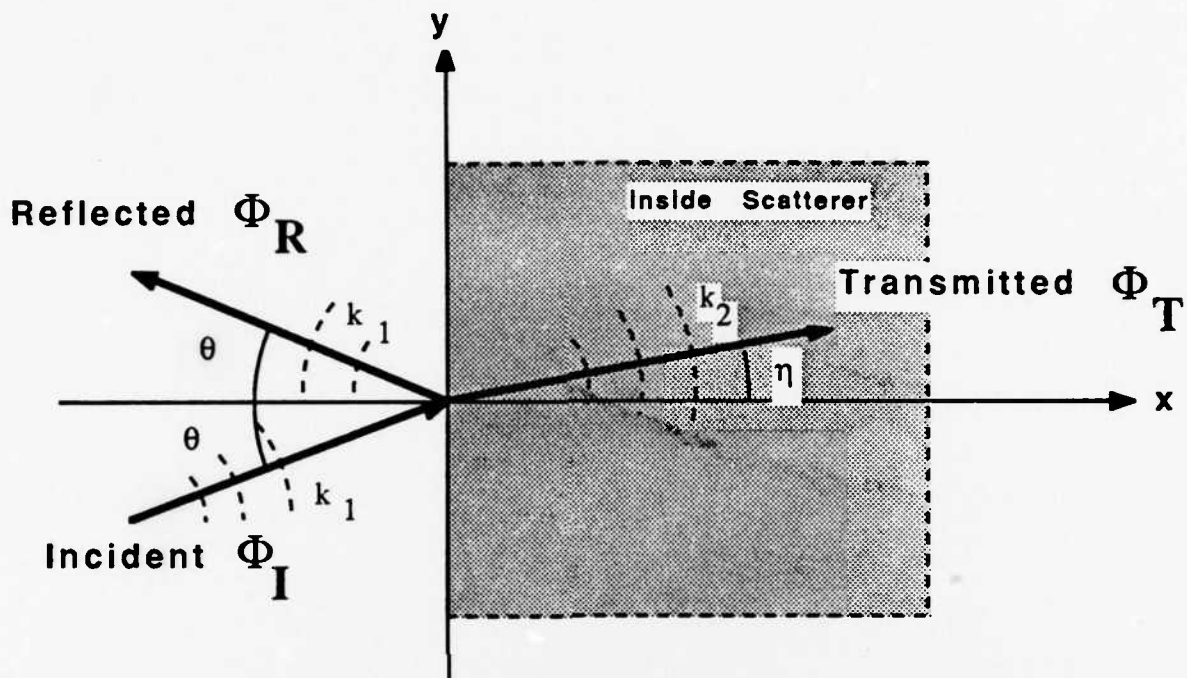


FIGURE B-1. INCIDENT, REFLECTED AND TRANSMITTED WAVES IN SCATTERING FROM A HALF-PLANE

DISTRIBUTION

	<u>Copies</u>		<u>Copies</u>
Commander		Internal Distribution:	
Naval Ocean Systems Center		E231	2
Attn: Technical Library	1	E232	15
San Diego, CA 92152		U202 (T. Ballard)	1
		U04 (M. Stripling)	1
Commanding Officer		U042 (J. Bilmanis)	1
Naval Underwater Systems		U05 (R. Stevenson)	1
Center		U25 (L. Barkakati)	5
New London Laboratory		U25 (S. Hebbert)	5
Attn: Technical Library	1	U25 (J. Arvelo)	1
New London, CT 06320		U25 (M. Williams)	1
		U25 (P. Jackins)	1
Defense Technical Information			
Center			
Cameron Station			
Alexandria, VA 22304-6145	2		

END
FILMED

6-89

DTIC